HHS Public Access

Author manuscript

Mater Lett. Author manuscript; available in PMC 2019 April 15.

Published in final edited form as:

Mater Lett. 2018 April 15; 217: 27–32. doi:10.1016/j.matlet.2017.12.147.

Development of a Novel Loading Device for Studying Magnesium Degradation under Compressive Load for Implant Applications

Qiaomu Tian[1], **Jose Antonio Mendez**[1,2], **Laura Rivera-Castaneda**[1], **Omar Mahmood**[1], **Adam Showalter**[1], **Elizabeth Ang**[1], **Sarah Kazmi**[1], and **Huinan Liu**[1,3,*]

[1]Department of Bioengineering, University of California, Riverside. Riverside, CA, USA, 92521

[2]Department of Mechanical Engineering, University of California, Riverside. Riverside, CA, USA, 92521

[3]Materials Science and Engineering, University of California, Riverside. Riverside, CA, USA, 92521

Abstract

Medical implants play a key role in treating bone fractures. Permanent implants are currently used for immobilization of fractures and bearing physiological loads during bone healing. After bone has healed, these implants, if not removed, often cause complications in the long run; and secondary surgeries for removing them pose additional discomfort and expenses for patients. Magnesium (Mg)-based bioresorbable implants, can potentially eliminate the need for additional surgeries by degrading safely over time in the human body. When studying the degradation behaviors of Mg-based implants *in vitro*, it is important to simulate physiological conditions *in vivo* closely, including loading. Considering that implants often carry physiological loads *in vivo* and mechanical stresses affect the degradation rate of Mg, a novel loading device was designed and manufactured for studying Mg degradation under load over a long period of time in a simulated body fluid *in vitro*. Degradation of Mg rods were investigated by immersing in a revised simulated body fluid (rSBF) for two weeks while a consistent compressive load was applied using the loading device. The results showed that the loading device provided a consistent load of 500 ± 45 N during the two weeks of immersion. Mg rods showed a significant faster degradation rate under the applied load, as demonstrated by a higher mass loss of the sample, a higher pH increase and Mg^{2+} ion release in the rSBF.

Graphical abstract

*Corresponding Author: Huinan Liu, Ph.D., Associate Professor, Department of Bioengineering, Materials Science and Engineering Program, University of California at Riverside, 900 University Avenue, Riverside, CA 92521, Office: MSE 227, Phone: 951 827 2944, Fax: 951 827 6416, huinan.liu@ucr.edu.

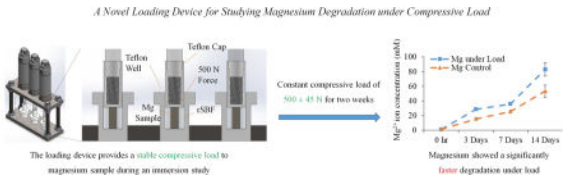

Keywords

Biomaterials; magnesium-based biodegradable metals; corrosion; degradation; loading device; load bearing bioresorbable implants

1. Introduction

Magnesium (Mg) has great potentials to serve as next-generation bioresorbable implants for medical applications due to their excellent mechanical properties, biodegradability, and biocompatibility [1, 2]. Biodegradability of Mg-based implants and interactions with relevant cells have been studied *in vitro* for orthopedic and urological applications [3, 4]. Most of the *in vitro* studies on the degradation of Mg-based implants were performed by immersion in physiologically relevant fluids at the body temperature of 37°C to represent the chemical and thermal environment *in vivo*. It is desirable to include physiological loading as one of the key contributing factors when studying *in vitro* degradation of Mg-based metals for medical implant applications, because mechanical stress could increase the corrosion rates of Mg-based alloys and composites [5–7]. For example, cyclic loading significantly increased the corrosion rates of high purity magnesium (99.99 wt.%), binary Mg-1Ca, and ternary Mg–2Zn–0.2Ca alloys in simulated body fluid (SBF) [5]. Li et al. reported that the degradation of Mg/Poly (Latic acid) wires was accelerated under a dynamic compressive stress of 0.9 MPa at a frequency of 2.5 Hz [6, 7]. Mg-based alloys are known to be susceptible to stress corrosion cracking (SCC); and Mg-based implants may degrade faster and experience sudden fracture under load, especially in a humid environment such as inside the body [8, 9]. Mechanical behaviors of Mg have been investigated using a slow rate test (SRT) method in modified simulated body fluid, and Mg did show a lower elongation and ultimate tensile strength due to SSC [10, 11]. Thus, it is important to study the degradation behaviors of Mg-based implants under load for a long period of time, preferably weeks to months, to understand the properties of these implants as they degrade. Although *in vivo* studies in animal models can provide complimentary information about the performance of Mg-based implants under load, the load in small animal models, such as rats, cannot be directly translated to the human study due to the significant differences in musculoskeletal structures between small mammals and human. Before clinical studies, large animal models, such as sheep and dogs, are often recommended for evaluating orthopedic implants because they have similar loading conditions as human [12, 13]. However, long-term studies in large animal models are always costly and involving sacrifice of many animals. Therefore, the objective of this study was to develop and build a novel loading device to simulate the human-like physiological loading conditions *in vitro* for studying biodegradable implants in a long period of time from weeks to months. The degradation behaviors of Mg rods under applied loads of 500 N were investigated for up to

two weeks using this loading device. This study demonstrated the effects of physiologically relevant loading on Mg degradation.

2. Device Design and Experimental Methods

2.1. The Design and Development of the Loading Device

Figure 1 shows the schematic design for the loading device. The loading device was designed to be able to apply variable load onto the implant materials during immersion degradation testing *in vitro*. The device contains three major parts: power supplier (Figure 1a), loading chambers (Figure 1b, c), and electrical components (Figure 1d, e). Specifically, the air compressor (Figure 1a) sends compressed air to extend the pneumatic pistons (Figure 1b), thus applying a load onto the Mg rods. The load can be adjusted by controlling the air pressure, and the loading force is read by the load cell (Figure 1c) and is transmitted to an Arduino Uno (Figure 1d). The Arduino Uno sends the data to the Raspberry Pi 3B (Figure 1e) where the data are stored and displayed on a monitor in real time.

An implementation of the whole loading device is illustrated in Figure 2. The air compressor (C2002, Porter Cable, TN, USA), as the power supplier, provides compressed air which ranges from 0 psi to 200 psi to the piston. The loading device contains three pneumatic pistons (4952K354, McMaster-Carr, CA, USA) placed in a frame, which was machined out of stainless steel (McMaster-Carr, CA, USA), and 3D printed out of Poly lactic acid filament (PLA, Makerbot, NY, USA) using a MakerBot Replicator (MakerBot Replicator Desktop 3D Printer, MakerBot, NY, USA). The design of triplicate loading chambers is to accommodate triplicate samples in a single test. The pistons are made out of stainless steel, have a bore size of one and half inches, and can each output a load up to 1500 Newton of force by regulating the output pressure of the air compressor. The output force of the pistons is determined by the following Eq. 1.

$$F=\rho A=\rho\pi d^2/4 \quad (1)$$

Where F is the force exerted, ρ is the gauge pressure, A is the full bore area, and d is the full bore piston diameter. Each piston contains two intake valves (Figure 2b) for air to flow in and to control the extension of the piston. Screws were threaded into tubing and inserted into one of the two intake valves to help prevent air from leaking. Levels were placed on the frame of the loading device to ensure the pneumatic pistons were perpendicular to the bottom plate, and apply a vertical force onto the Mg rod (Figure 2b). A load cell (TAS606, Sparkfun, CO, USA) is positioned underneath the middle well. The load cell is capable of reading a maximum of 200 kg.

The electrical components include a load cell amplifier, an Arduino Uno, and a Raspberry Pi. Specifically, the load cell amplifier provides a stronger signal with less noise (i.e., a higher signal to noise ratio) to the Arduino Uno for accurate data collection (Figure 2c). Arduino Uno (Arduino Uno, Arduino, Turin, Italy) functions as the microcontroller powering both the load cell and the load cell amplifier (Figure 2c). The Arduino collects the force data received from the load cell amplifier and transmits that to the Raspberry Pi. The

Arduino Uno was chosen for its ease of implementation as it can be rapidly applied and modified through its hardware, and programing. A Raspberry Pi (Raspberry Pi 3B, Raspberry Pi, Cambridge, United Kingdoms) is connected to the Arduino Uno to display the force values on a monitor. Adding the Raspberry Pi 3B allows for streaming and storing of the data of the actual load applied to the Mg-based implant *in situ*. The Raspberry Pi 3B was selected as a more cost effective solution to run the programming code and to store the data received from the Arduino Uno instead of using a desktop or laptop. By storing the data and displaying them in real time, the user can monitor the accuracy of the loading device without being present for the full duration of the degradation study, which can range from weeks to months.

2.2. Degradation of Mg Rods in rSBF with Applied Load versus No Load

Mg rods (99.95%, GalliumSource, CA, USA) were cut into 15 mm × 6 mm using a handsaw, and then polished using silicon carbide papers (SiC, Ted Pella Inc., Redding, CA, USA) from 600 grit to 1200 grit. The polished samples were degreased and cleaned in acetone (Sigma Aldrich, St Louis, MO, USA) for 30 min and in 100% ethanol (Sigma Aldrich, St Louis, MO, USA) for 30 min respectively, using an ultrasonic cleaner (Model 97043-936, VWR, Radnor, PA, USA). Before immersion, all of the Mg samples were weighed using an analytical balance (Ms104S, Mettler Toledo, Columbus, OH, USA), and the mass of each sample was recorded as the initial mass (M_o).

The well design of the loading chamber for housing the Mg samples is shown in Figure 3. To prevent the galvanic corrosion between the Mg samples and the piston, the wells and the caps on the pistons (Figure 3b) were machined out of Teflon to avoid the metal to metal contact. The Mg rod samples were placed into Teflon wells and immersed in 2.5 mL of revised simulated body fluid (rSBF) that has the same ionic composition as human blood plasma [14]. A load of 500 N was applied on each Mg rod at room temperature until the prescribed immersion time point is reached. The Mg rod controls were also placed in the Teflon wells respectively and immersed in 2.5 mL of rSBF but without load. The Mg rod samples were immersed in rSBF for 3 days, 1 week, and 2 weeks. The rSBF was replenished every other day. The immersion degradation experiment was run in triplicate concurrently.

After each immersion period, the rSBF was collected from the wells and the Mg rod samples were dried in a vacuum (Multipurpose Vacuum Oven, Thermo Scientific, MA, USA) at room temperature. The macroscopic images of the dried Mg rod samples that were tested with or without 500 N of load were taken using a camera (Model SX500 IS, Cannon). The dried Mg samples were also weighed using an analytical balance to determine the final mass (M_f) after immersion. The mass change (%) of Mg samples at different time points was then calculated following the equation $(M_f - M_o)/M_o$, where M_f is the final mass and M_o is the initial mass. The pH of the collected rSBF was measured using a pH meter (SB70Pm, SympHony, PA, USA). The Mg^{2+} ion concentrations were quantified using inductively coupled plasma - optical emission spectrometry (ICP-OES; Optima 8000, Perkin Elmer, MA, USA). Briefly, the collected solutions from each well were diluted with deionized (DI) water by a factor of 1:100 into a total volume of 10 mL. Mg^{2+} ion concentrations were then quantified based on the calibration curves generated using Mg^{2+} standards (Perkin Elmer)

serially diluted to a concentration of 0.5, 1, 2, and 5 mg/L. The characterization process was repeated for each time point.

2.3. Statistical Analysis

Since the data met assumptions of normal distribution and homogeneity of variances, a one-way analysis of variance (ANOVA) was used to examine the statistical difference among all the groups. Tukey post-hoc test was used for detecting statistical differences when comparing between two groups. All graphs represent average values ± standard deviation. A statistically significant difference was considered at $p < 0.05$.

3. Results

3.1. Surface Morphology and Mass Change of the Mg Samples

The macroscopic images of the Mg under load and Mg controls without load showed different surface morphologies after 14 days of immersion in rSBF (Figure 4a). Generally, all the Mg samples showed deposition of degradation products after 3 days of immersion. The white degradation products increased as the time increased during the immersion. Mg rods under load, however, had a less degradation products on the surface than that of Mg controls, especially at 7 days and 14 days. Figure 4b shows the mass change of the Mg under load and Mg controls after 14 days of immersion in rSBF. Statistically significant difference was found among the Mg-based samples during the 11 days of immersion [$F(6,17)=175.7$, $p<0.0001$]. All the Mg samples had a significant mass decrease after the immersion. At the 3 days of immersion, all the Mg samples had a mass increase due to the deposition of the degradation products. The Mg under load showed a higher mass increase than the Mg controls. Starting at 7 days of immersion, all the Mg samples had a significant mass decrease, where the Mg under load showed a significantly higher mass loss than the Mg controls. At 14 days of immersion, the mass of Mg controls had no significant change in comparison with the previous time point. The mass of Mg under load, however, showed a mass loss which was significantly lower than the Mg controls.

3.2. Analysis of the rSBF after Immersion Degradation

Figure 4c displays the pH of the rSBF for the Mg under load and Mg controls after 14 days of immersion. Statistically significant difference was found among the Mg-based samples during the 11 days of immersion [$F(6,17)=10.86$, $p=0.004$]. Generally, the pH of Mg-based samples showed an increasing trend as time increased during the immersion. When comparing the Mg under load and Mg controls without load, the pH of Mg controls was higher than that of Mg under load at 3 days and 7 days of immersion. The pH of Mg controls at 14 days, however, showed a lower pH than the previous time point, possibly because the continuous deposition of degradation products slowed the degradation of Mg samples. At 14 days of immersion, the pH of Mg controls was significantly lower than that of Mg under load. From Figure 4d, the Mg^{2+} ion concentration of the rSBF for the Mg rods under load and Mg controls showed a significant increase during the 14 days of immersion. Statistically significant difference was found among the Mg-based samples during the 11 days of immersion $F(6,17)=55.82$, $p<0.0001$]. The Mg^{2+} ion concentrations of Mg-based samples showed an increasing trend as time increased during the immersion. The Mg under load

showed a higher Mg^{2+} ion concentration in average than that of Mg controls at all-time points during the immersion. Statistical difference was found at 3 days of immersion and 14 days of immersion.

4. Discussion

Engineering the loading device for studying Mg-based biomaterials *in vitro* involves three major challenges, that is, automating, powering, and downscaling in size. Although the current version of our loading device meets the critical design criteria and functional requirements for studying Mg degradation under load, further improvements in the following aspects are still recommended to make the device more user friendly and more robust for repeated experiments. First, automating operation of the loading device can greatly improve the repeatability of experimental results and benefits the users especially in the long-term studies that span from weeks to months. The current pneumatic pistons are powered through an air compressor, which needs to be manually adjusted by the user due to natural accruing air leaks in the system. To improve this, the pneumatic powered pistons can be replaced with electrically powered pistons, and a feedback or closed loop control system can be added for autonomous regulation. One piston type of interest would be hydraulic pistons as they are small, and able to output large forces that would be required for testing various medical implant material. Using these electrical powered pistons, a feedback loop can be created through various means, such as using electrical components that read the output force of the electrical powered pistons, and with that data the device could self-correct itself to the desired load output without the need of a user. To implement this, a self-adjusting controller such as a PID controller, would be able to provide the device with both versatility and higher accuracy.

Second, the device should simulate the body conditions more closely during the *in vitro* experiments in addition to applying a load onto the implant material. Specifically, it is beneficial to conduct the experiments under standard cell culture conditions inside an incubator, i.e., a sterile, 37°C, 5% CO_2/95% air, humidified environment, because such environment resembles the conditions inside the body. The power system of our current device, i.e., outlet, is not ideal for most standard incubators, because it requires cords coming out of the incubator and causes a concern on maintaining the environmental parameters inside an incubator. To address these issues, the loading device could have its own built-in source of power such as a battery. The battery should be able to provide enough power that allows the device to run for the full duration of the study that could last from weeks to months. Considering that the standard environment inside an incubator involves heat and humidity, a proper shield system would have to be incorporated to protect the battery and electrical components.

Third, downscaling the overall size of the device is another important aspect of future improvement, because smaller size would allow the device to be more portable and easier to be placed inside a standard incubator. As aforementioned, the hydraulic pistons and the battery can significantly reduce the overall size of the device due to the smaller size of each component and elimination of using an air compressor. Other electrical components, such as the Arduino Uno and Raspberry Pi, can be integrated into one to reduce the overall size as

well. The possible drawback of these improvements is the increased cost for the device. The current first-generation loading device was designed and built with a small budget of a few hundred dollars, and demonstrated its functionality successfully in studying the degradation of Mg rods in rSBF under load.

Conclusions

The loading device was successfully designed and developed, and provided consistent load of 500 ± 45 N during a two-week immersion study with Mg rods. Future improvements, such as automating, powering, and downscaling in size, are recommended to explore the full potential of the loading device for *in vitro* degradation testing of biodegradable implant materials. The Mg rods under load showed a significant faster degradation than that under no load, as demonstrated by a higher mass loss of the sample, a higher pH increase and Mg^{2+} ion release in the rSBF. It is recommended to evaluate *in vitro* degradation of Mg-based biodegradable implants under load, because it resembles physiological conditions more closely. With further improvements, the loading devices may be useful to bridge the gap between the results from *in vitro* degradation and *in vivo* degradation of Mg-based biomaterials, potentially reducing the number of animals needed for biodegradable implant research.

Acknowledgments

The authors would like to thank the U.S. National Science Foundation (NSF award 1512764, 1125801), Hellman Fellowship (H.L.), University of California (UC) Regents Faculty Development Award (H.L.), UC Riverside Graduate Dean's Dissertation Research Grant (Q.T.), Hispanic Serving Institution for Undergraduate Research Program (J.M.) and Maximizing Access to Research Careers Undergraduate Student Training in Academic Research (MARC U STAR) Pre-Trainee Program (J.M.) for financial support. The authors would like to thank Peter Hung for the help with Python code writing. The content is solely the responsibility of the authors and does not necessarily represent the official views of the National Science Foundation.

References

1. Staiger MP, Pietak AM, Huadmai J, Dias G. Magnesium and its alloys as orthopedic biomaterials: a review. Biomaterials. 2006; 27(9):1728–34. [PubMed: 16246414]
2. Gu X-N, Zheng Y-F. A review on magnesium alloys as biodegradable materials. Frontiers of Materials Science in China. 2010; 4(2):111–115.
3. Tian Q, Deo M, Rivera-Castaneda L, Liu H. Cytocompatibility of Magnesium Alloys with Human Urothelial Cells: A Comparison of Three Culture Methodologies. ACS Biomaterials Science & Engineering. 2016
4. Iskandar ME, Aslani A, Tian Q, Liu H. Nanostructured calcium phosphate coatings on magnesium alloys: characterization and cytocompatibility with mesenchymal stem cells. Journal of materials science. Materials in medicine. 2015; 26(5):189. [PubMed: 25917827]
5. Bian D, Zhou W, Liu Y, Li N, Zheng Y, Sun Z. Fatigue behaviors of HP-Mg, Mg-Ca and Mg-Zn-Ca biodegradable metals in air and simulated body fluid. Acta Biomater. 2016; 41:351–60. [PubMed: 27221795]
6. Li X, Chu C, Chu PK. Effects of external stress on biodegradable orthopedic materials: A review. Bioactive Materials. 2016; 1(1):77–84.
7. Li X, Qi C, Han L, Chu C, Bai J, Guo C, Xue F, Shen B, Chu PK. Influence of dynamic compressive loading on the in vitro degradation behavior of pure PLA and Mg/PLA composite. Acta biomaterialia. 2017; 64:269–278. [PubMed: 28782722]

8. Song RG, Blawert C, Dietzel W, Atrens A. A study on stress corrosion cracking and hydrogen embrittlement of AZ31 magnesium alloy. Materials Science and Engineering: A. 2005; 399(1–2): 308–317.

9. Winzer N, Atrens A, Song G, Ghali E, Dietzel W, Kainer KU, Hort N, Blawert C. A critical review of the stress corrosion cracking (SCC) of magnesium alloys. Advanced Engineering Materials. 2005; 7(8):659–693.

10. Choudhary L, Singh Raman RK, Hofstetter J, Uggowitzer PJ. In-vitro characterization of stress corrosion cracking of aluminium-free magnesium alloys for temporary bio-implant applications. Mater Sci Eng C Mater Biol Appl. 2014; 42:629–36. [PubMed: 25063163]

11. Kannan MB, Raman RK. In vitro degradation and mechanical integrity of calcium-containing magnesium alloys in modified-simulated body fluid. Biomaterials. 2008; 29(15):2306–14. [PubMed: 18313746]

12. Smit TH. The use of a quadruped as an in vivo model for the study of the spine – biomechanical considerations. European Spine Journal. 2002; 11(2):137–144. [PubMed: 11956920]

13. Wilke HJ, Kettler A, Claes LE. Are sheep spines a valid biomechanical model for human spines? Spine (Phila Pa 1976). 1997; 22(20):2365–74. [PubMed: 9355217]

14. Iskandar ME, Aslani A, Liu H. The effects of nanostructured hydroxyapatite coating on the biodegradation and cytocompatibility of magnesium implants. Journal of Biomedical Materials Research Part A. 2013; 101A(8):2340–2354.

Highlights

- Designed a novel loading device for studying magnesium based implant materials under compressive load.
- The loading device is reliable and can provide a load range from 100 N to 1500 N for a long period.
- Magnesium showed a significantly faster degradation in simulated body fluid under a compressive load.

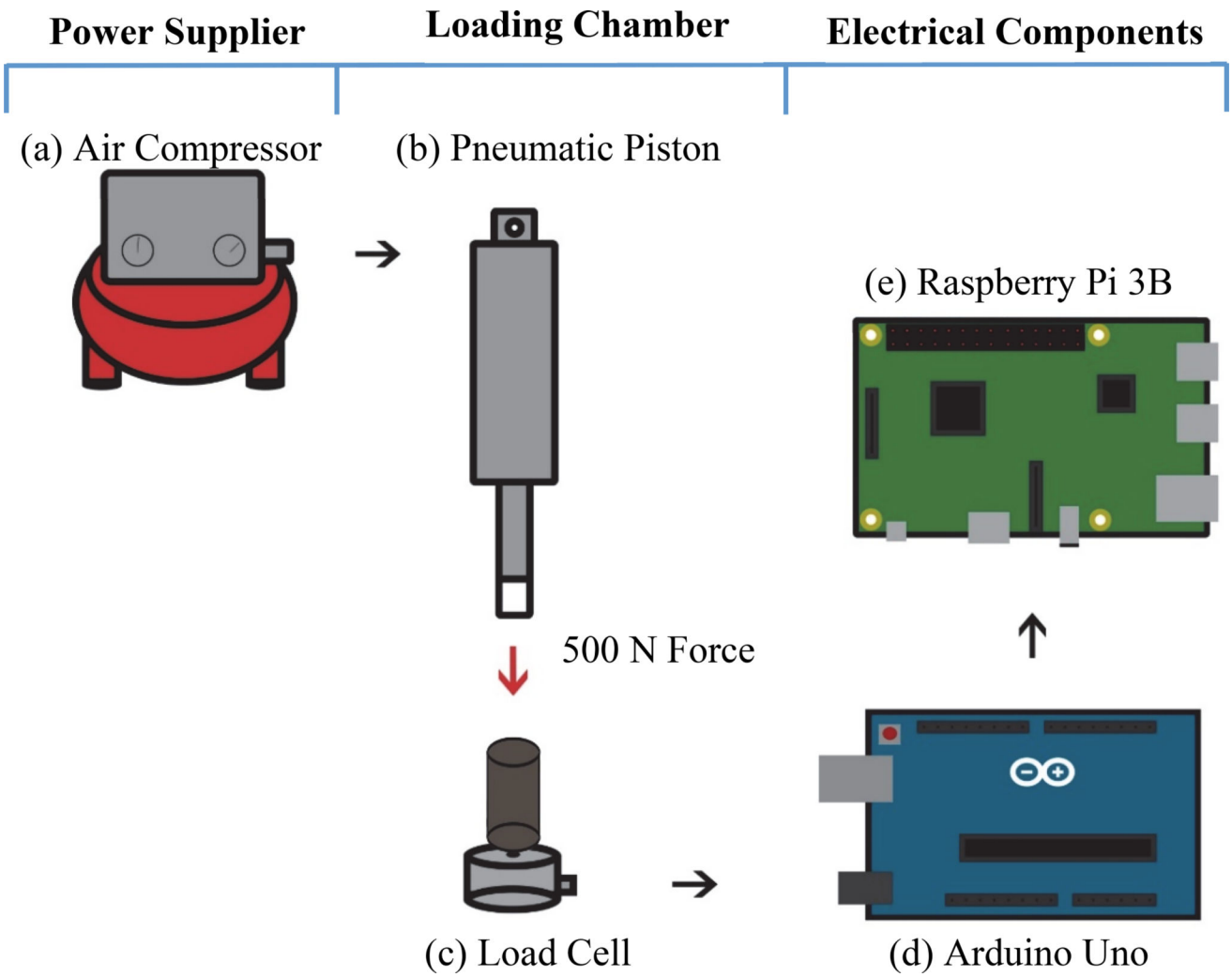

Figure 1.

The schematic design for the loading device, which contains three major components, i.e., power supplier (a), loading chamber (b, c), and electrical components (d, e). Specifically, (a) air compressor sends compressed air to extend the pneumatic piston. (b) The pneumatic piston applies the load onto the Mg rod. (c) Load cell that reads up to 200 kg and gathers the load applied to the Mg rod. (d) Arduino Uno powers the load cell and amplifier, and gathers the applied force from the load cell and amplifier, and then transmits it to the Raspberry Pi 3B. (e) Raspberry Pi 3B collects, stores, and streams the data transmitted from the Arduino Uno in real time.

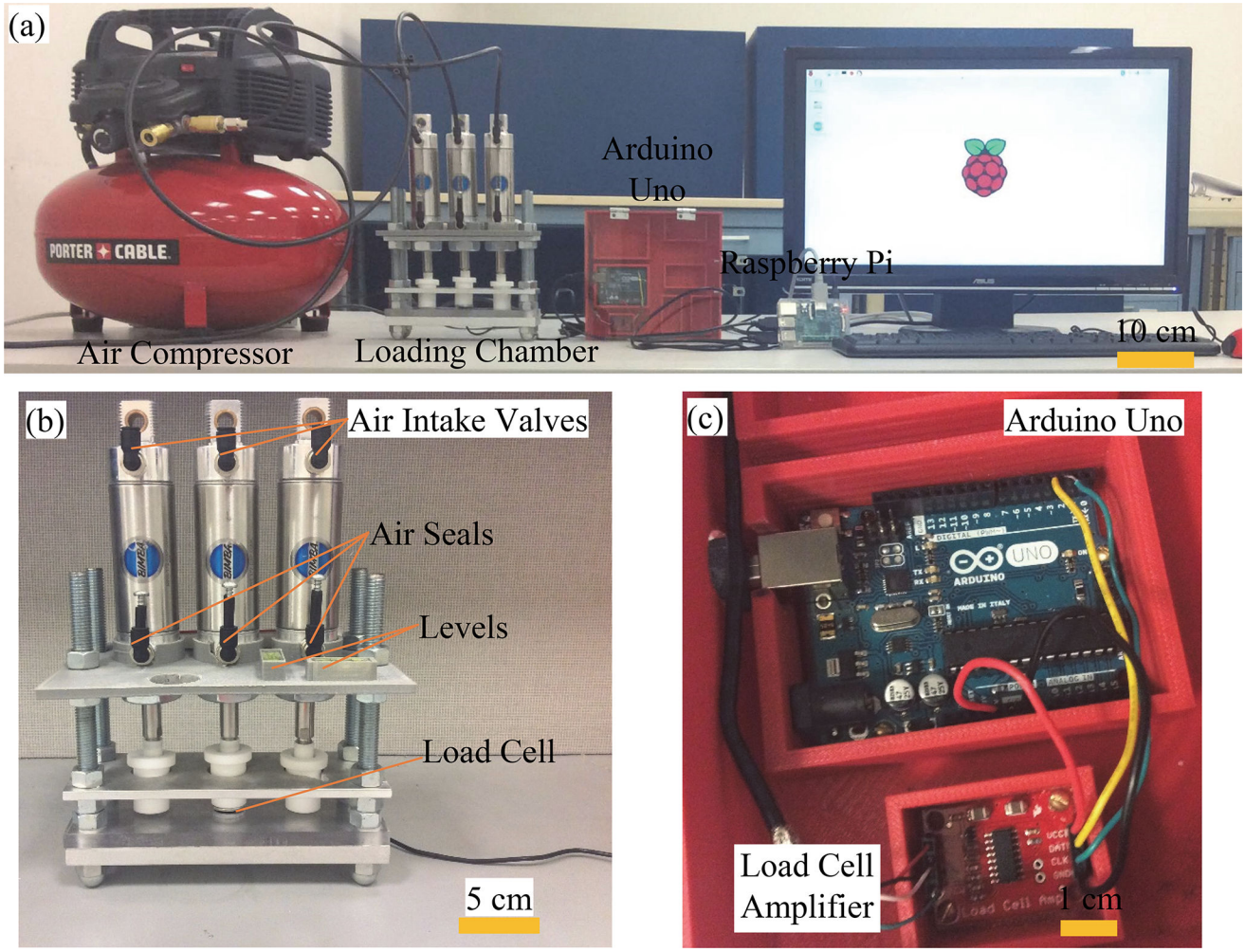

Figure 2.

The implementation of the actual loading device. (a) A general overview of the loading device and all of its components. (b) A detailed view of the loading chambers. The design of triplicate loading chambers allows simultaneous testing of triplicate samples. Air intake valves allow the air from the air compressor to extend the pneumatic piston and air seals prevent the incoming air from leaking out of the pistons. Two levels are used to ensure that the pistons are set up to apply a vertical force onto the Mg rod. A load cell is positioned underneath the middle Teflon well. The sample will be placed in the Teflon well during the immersion degradation study. (c) The electrical components of the device are the microcontroller, Arduino Uno that gathers and sends the force data to the Raspberry Pi 3B, and the load cell amplifier that amplifies the signal received from the load cell for the Arduino to read accurately. The scale bars are 10 cm, 5 cm and 1 cm for (a), (b), and (c) respectively.

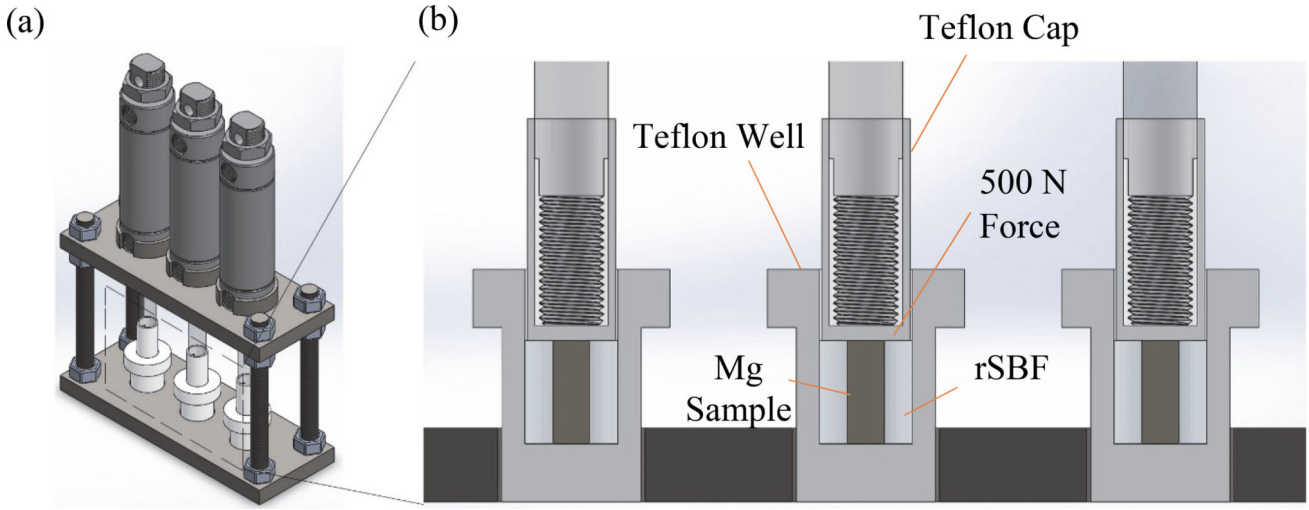

Figure 3.

The illustration of the loading chamber in SolidWorks. (a) An isometric view showing the assembly of loading chamber. (b) A cross-section view of the loading chamber detailing the well design. The cap and well were machined out of Teflon instead of metals to prevent direct metal-to-metal contact with Mg-based samples and consequent galvanic corrosion.

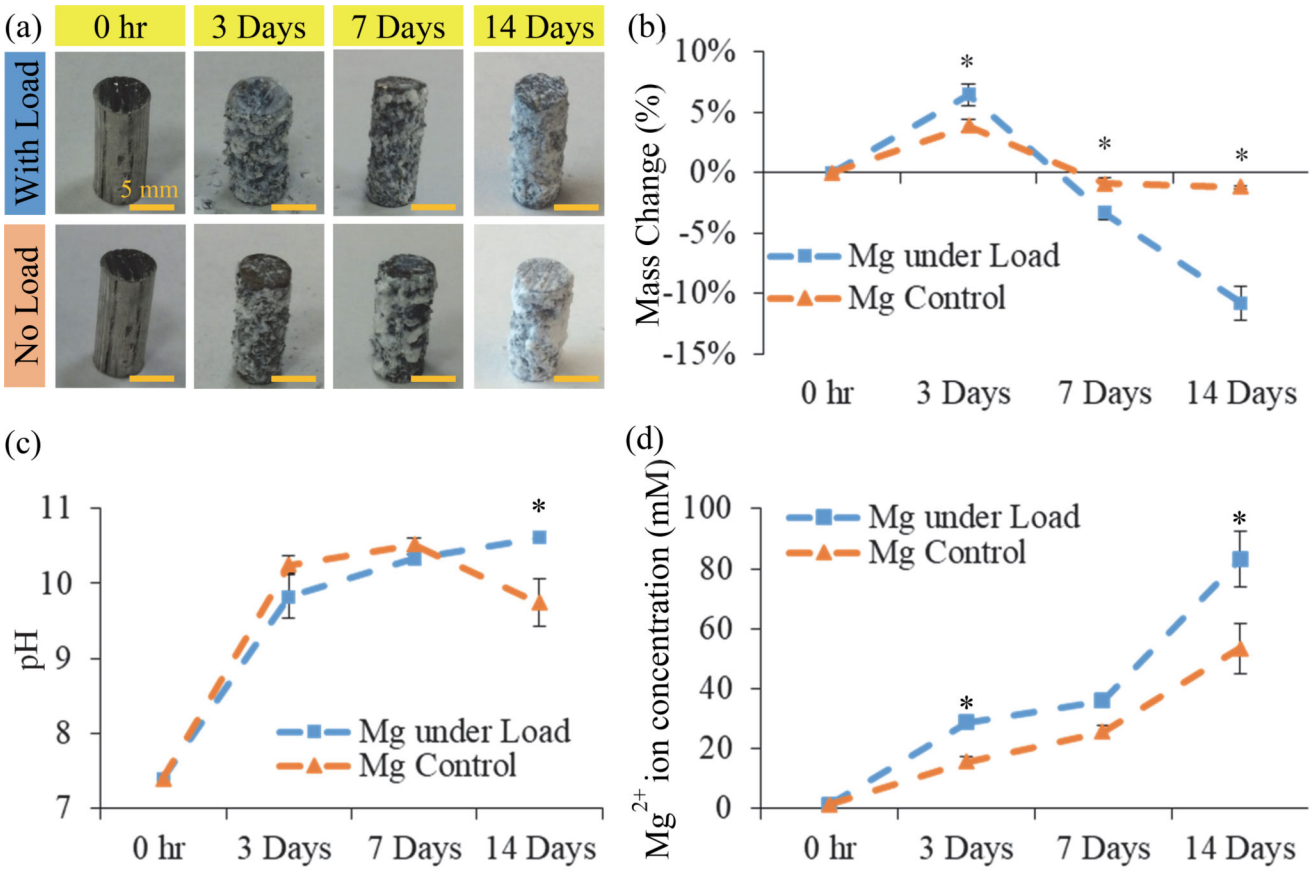

Figure 4.

The degradation behaviors of Mg rods under a compressive load of 500 N versus no load (i.e. Mg control) during the immersion degradation testing in rSBF. (a) Macroscopic images of the Mg rods with load versus no load at different time points of degradation study. Scale bars = 5mm. (b) Mass change of the Mg rods under load and Mg controls under no load in rSBF at different time points of degradation study. (c) The pH of rSBF after culture with Mg rods under load and Mg controls under no load at different time points of degradation study. (d) The Mg^{2+} ion concentrations in rSBF after culture with Mg rods under load and Mg controls under no load at different time points of degradation study. Data are mean ± standard deviation (N=3); *p<0.05.